Failure Properties of Thermoplastic Elastomers from Polyethylene/Nitrile Rubber Blends: Effect of Blend Ratio, Dynamic Vulcanization, and Filler Incorporation

Josephine George,[1] N. R. Neelakantan,[2] K. T. Varughese,[3] Sabu Thomas[1]

[1]*School of Chemical Sciences, Mahatma Gandhi University, Priyadarshini Hills P.O., Kottayam, Kerala 686 560, India*
[2]*High Polymer Engineering Division, Department of Chemical Engineering, Indian Institute of Technology, Chennai 600 036, India*
[3]*Polymer Laboratory, Central Power Research Institute, Bangalore 560 080, India*

Received 24 February 2003; accepted 3 September 2004
DOI 10.1002/app.21381
Published online in Wiley InterScience (www.interscience.wiley.com).

ABSTRACT: Thermoplastic elastomers from blends of high-density polyethylene and acrylonitrile butadiene rubber were prepared by a melt-blending technique. The blends were dynamically vulcanized using sulfur, peroxide, and mixed curing systems. The peroxide concentration was varied to obtain samples of varying degrees of crosslinking. The peroxide system showed better mechanical properties. The crosslink density determination by the equilibrium swelling method revealed that the enhancement in properties can be correlated to the extent of crosslinking. It is observed that the effect of dynamic vulcanization on the property improvement is much more pronounced in rubber-rich blends. To study the effect of filler incorporation on mechanical properties, fillers such as carbon black, silica, silane-treated silica, and cork-filled samples were prepared. All filled systems, except cork filled, exhibited superior mechanical properties. Scanning electron micrographs of selected fractured surfaces were analyzed to study the failure mechanism of the different compositions. Various theoretical models were applied to correlate the observed mechanical behavior with that of theoretically predicted values. © 2006 Wiley Periodicals, Inc. J Appl Polym Sci 100: 2912–2929, 2006

Key words: thermoplastic elastomer; vulcanization; mechanical properties; crosslinking; theoretical models

INTRODUCTION

Polymer blending is one of the easiest and most widely used techniques to prepare polymeric materials with desired properties. Blending a rubber with a plastic results in thermoplastic elastomers (TPEs). TPEs can be processed like a thermoplastic yet they possess the properties of vulcanized elastomers. Thus TPEs bridge the gap between plastic and rubber industries. One major drawback that limits the widespread acceptance of such systems is the incompatibility between the phases, resulting in premature failure.

It is well known that the properties of polymer blends depend on the morphology. One favorable morphology of thermoplastic elastomers is the formation of a large number of finely dispersed uncrosslinked or lightly crosslinked rubber particles in a small amount of the plastic phase, which is just sufficient to retain its flowability. Such a morphology can be achieved either by the use of a compatibilizer or by the process known as dynamic vulcanization. In the first case a block or graft copolymer, having segments identical to the component polymers, is used. The compatibilizer can be formed *in situ* or can be prepared separately and then added to the system to be compatibilized. Several excellent reviews on the compatibilization of polymer blends exist.[1–6] A block or graft copolymer locates at the interface and thereby reduces the interfacial tension, identical to the way by which an emulsifier acts.

Datta and coworkers[7,8] described the compatibilization of poly(styrene-*co*-maleic anhydride)/poly(ethylene-*co*-propylene) (SMA)/(EPM) blends by the addition of primary amine-modified EPM (EPM–NH_2) containing 0–3 mol % amine. A substantial improvement in notched Izod impact strength was reported. The improvement in impact strength can be correlated to the formation of imide bonds that have been proved by IR spectroscopy. These authors also reported that a significant amount of functionalized EPM can be replaced by nonfunctionalized high-density polyethylene (HDPE) without a detrimental loss of impact strength.

The success of compatibilizers has been demonstrated in the studies of several immiscible blend systems.[9–14] Okada et al.[15] reported on the morphological, thermal, and mechanical properties of blends of

Correspondence to: S. Thomas (sabut@md4.vsnl.net.in).

nylon 6 with maleated ethylene–propylene rubber. In this case the reaction of the polyamide amine end group with the grafted maleic anhydride resulted in TPEs with controlled morphology and chemical bonding between the phases.

Inferior mechanical properties of compatibilized blends, compared to noncompatibilized blends, has been ascribed to the macrophase separation of the compatibilizer.[16,17] If the compatibilizer has poor mechanical properties in the pure state, phase separation may lead to inferior mechanical properties. When a compatibilizer improves the interfacial adhesion and phase dispersion in a blend, and at the same time has adverse effects on either or both phases, the resulting mechanical properties of the blend are determined by a combination of the two factors.[16]

The more physical approach toward compatibilization for TPEs is by the use of dynamic vulcanization. The principle of dynamic vulcanization is to crosslink the rubber phase during its melt mixing with the plastic. For blends with similar polarities, a fine morphology is frozen in during dynamic vulcanization. However, a coarse morphology is developed in the case of incompatible blends.[6]

Several articles are quoted in the literature[18–22] on the dynamic vulcanization of rubber/plastic blends. Dynamic vulcanization of polypropylene (PP)/EPDM by sulfur[18] resulted in a dramatic improvement in tensile strength and elongation at break and a reduction in tension set with increase in sulfur content up to 2 phr. However, a sulfur system is not used commercially for PP/EPDM blends because PP has a high melting point and the crosslinks lack thermal stability. The dynamic vulcanization of PP/EPDM blend by resoles[19] resulted in improvement in tensile strength and elongation at break. The main reasons for using resoles are their activities at temperatures above 200°C and the formation of thermally stable carbon–carbon bonds.

The blend system under discussion consists of high-density polyethylene (HDPE) and acrylonitrile butadiene rubber (NBR). The very purpose of blending HDPE and NBR is to develop oil-resistant thermoplastic elastomers. The crystallinity of HDPE and the oil resistance of NBR make the system resistant to hot oils. Technological compatibilization is used to reduce the incompatibility problem.

The present article discusses the failure properties of HDPE and NBR blends. The effect of blend ratio and dynamic vulcanization on the fracture behavior is analyzed. The effect of filler incorporation on mechanical properties is also brought under investigation. Attempt has been made to correlate the fracture behavior with the morphology of a few selected samples. Various theoretical models were analyzed to correlate the experimental result with that of the theory.

EXPERIMENTAL

High-density polyethylene (HDPE; density, 0.96 g/cm^3; melt flow index, 7.5 g/10 min) was supplied by M/s Indian Petrochemicals Corp. Ltd. (Baroda, India). Acrylonitrile butadiene rubber (NBR; density, 0.98 g/cm^3; acrylonitrile content, 32%) was procured from M/s Synthetics and Chemicals (Bareilley, UP, India). Fillers such as carbon black (N ′330), cork, silica, and treated silica were used. The particle sizes of carbon black and silica were 29 and 20 nm, respectively. Cork filler was of much higher particle size of the order of millimeters. Treatment of silica did not make any difference in particle size. The filler loading was based on the rubber content. Only in high rubber blends was the filler loading varied to study the reinforcement by the filler. First a rubber and filler masterbatch was made on a two-roll mill with all the ingredients except the curatives. The requisite quantity of the masterbatch was then added to the plastic while melt mixing to get the exact composition.

Our experiments revealed that dicumyl peroxide (DCP) is the best curative for NBR and in a previous article we reported[23] on the variation of crosslink density of HDPE/NBR blends with the dosage of DCP. The effect of crosslink density on mechanical properties is studied by varying the DCP dosage from 1 to 4 phr based on the rubber content. The DCP used was 40% active.

To get an idea about the type of crosslinks on the mechanical properties, different crosslinking systems were studied. The various crosslinking systems used include sulfur, DCP, and a combination of sulfur and DCP. The sulfur curing system consisted of sulfur 0.1 phr, tetramethyl thiuram disulfide (TMTD) 2.0 phr, and cyclohexyl benzthiazyl sulfenamide (CBS) 2.5 phr. The mixed curing system contained sulfur 0.05 phr, TMTD 1.0 phr, CBS 1.25 phr, and DCP 2 phr. Zinc oxide (ZnO) and stearic acid were used in the proportion 5 : 1 in all the mixes.

The melt mixing was carried out at 160°C at a rotor speed of 60 rpm. The mixing time was 6 min. First HDPE was charged into the mixer and allowed to melt. After 2 min, the rubber or the masterbatch was added and allowed to mix for 2 min. The curatives (if any) were added and mixed for 3 min in the case of vulcanized blends. The unvulcanized blends were mixed for 4 min.

The unvulcanized blends were represented by the letter H and the subscripts following it represent the amount of HDPE in the blend. Dynamic vulcanization using sulfur, dicumyl peroxide, and mixed curing systems were represented by the notations S, D, and SD, respectively. In filled systems C, K, Si, and TSi stand for carbon black, cork, silica, and treated silica, respectively, and the subscripts following each notation indicate the concentration of filler in the blend. Thus the

uncrosslinked and unfilled blends were represented by H_{100}, H_{70}, H_{50}, H_{30}, and H_0, depending on the blend ratio. In these, the subscripts indicate the weight percentage of HDPE in the blend. The notation for filled and dynamically vulcanized blend is explained using H_{50} blend as an example. Thus $H_{50}C_{30}D_4$ indicates a 50/50 blend of HDPE and NBR, containing 30 phr carbon black, crosslinked by 4 phr DCP.

Mechanical properties

Tensile testing was done according to the ASTM D412-80 test method using dumbbell-shape samples at a crosshead speed of 500 mm/min using a universal testing machine (Zwick 1465, Bamberg, Germany).

Tear strength was determined using unnicked 90°-angle test samples according to the ASTM D 624-81 test method. The testing speed was identical to that of tensile testing.

Scanning electron micrographs

SEM photomicrographs of tensile and tear fractured samples were taken after sputter coating the fractured surface with gold–palladium alloy. The morphologies of dynamically vulcanized samples were studied using liquid nitrogen fractured samples. Because the samples were crosslinked, the preferential extraction of the rubber phase was not possible. The samples were directly used without extraction and SEM micrographs were taken on a scanning electron microscope (model 500C; Philips, Eindhoven, The Netherlands). The domain dimensions were measured using an image analysis technique by considering a large number of particles.

Crosslink density determination

The molar mass between crosslinks (M_c) of dynamically vulcanized samples were determined by equilibrium swelling in toluene using the equation[24]

$$M_c = \frac{-\rho_p V_s V_r^{1/3}}{\ln(1 - V_r) + V_r + \chi V_r^2} \quad (1)$$

where ρ_p is the density of the polymer; V_s is the molar volume of the solvent; and V_r is the volume fraction of swollen rubber, which is given by

$$V_r = \frac{(d - f_1 w)\rho_p^{-1}}{(d - f_1 w)\rho_p^{-1} + A_s \rho_s^{-1}} \quad (2)$$

where d is the deswollen weight of the sample, f_1 is the volume fraction of insoluble component, w is the weight of sample, ρ_s is the density of the solvent, and A_s is the amount of solvent absorbed.

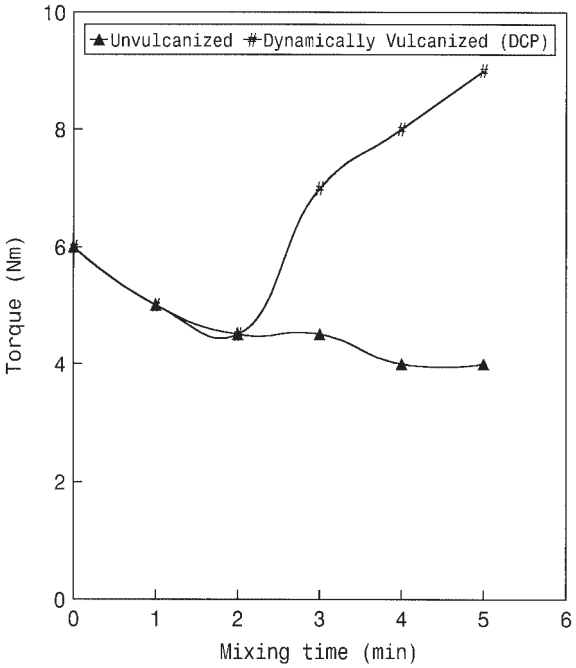

Figure 1 Typical Brabender plastographs showing the effect of dynamic vulcanization on the torque values of a 70/30 blend of HDPE and NBR.

The interaction parameter is given by[25]

$$\chi = \beta + \frac{V_s}{RT}(\delta_s - \delta_p)^2 \quad (3)$$

where β is the lattice constant (0.34); R is the gas constant; T is the absolute temperature, and δ_s and δ_p are the solubility parameters of the solvent and polymer, respectively. The crosslink density υ was calculated from M_c as

$$\upsilon = \frac{1}{2M_c} \quad (4)$$

RESULTS AND DISCUSSION

Brabender curves

Typical Brabender plastographs for unvulcanized and dynamically vulcanized (DCP cured) H_{70} are shown in Figure 1. In the unvulcanized sample, the torque decreases with mixing time and finally registers a constant value, indicating complete mixing of ingredients. In dynamically vulcanized samples, the mixing torque increases with mixing time, which is explained by the fact that the crosslinked rubber particles exert increased resistance to rotation, which in turn results in increased torque values.

The effect of DCP concentration on the final torque values of H_{70}, H_{50}, and H_{30} are shown in Figure 2.

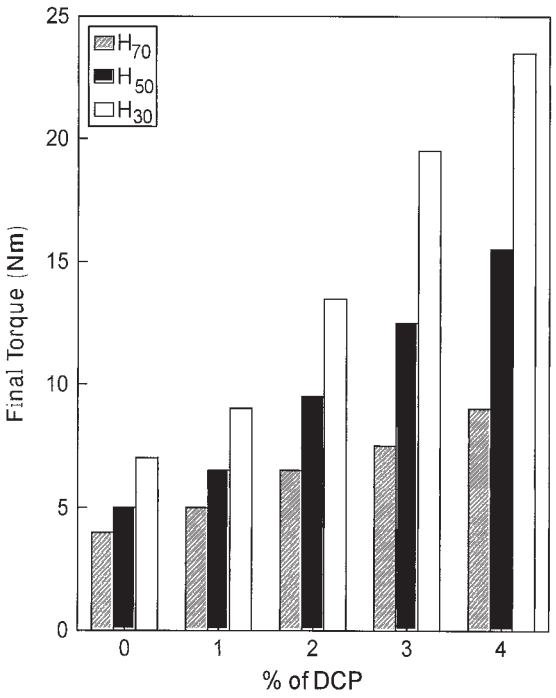

Figure 2 Bar graph showing the effect of DCP concentration on the final torque values of 70/30, 50/50, and 30/70 blends of HDPE and NBR.

From the figure it is very clear that the final torque values increase with DCP concentration. The effect of DCP on polyolefins is determined by the structure of the base polymer. Peroxide-initiated reactive extrusion of polyolefin may lead to oxidative degradation, crosslinking, or chain scission, depending on the type of polymer, compounding conditions, and partial pressure of oxygen.[26] With respect to the polymer, the structure of the pendant group (R) determines the preferred reaction pathway. In the case of polypropylene (PP), (R = CH_3), the positive induction effect of the methyl group facilitates a homolytic scission of the C—H bonds and the tertiary macroradical formed will readily undergo chain scission even under a low partial pressure of oxygen.

At high oxygen pressure, oxidative degradation predominates. In addition, the pendant methyl groups provide PP with steric hindrance for the coupling of two macroradicals. For polyethylene (PE) such an effect or hindrance does not exist, and thus crosslinking reactions by the combination of secondary macroradicals dominate.[27,28] Thus the increase in torque with DCP concentration in the present case is a result of the crosslinking of both the rubber and plastic phases. Also, it is evident that at a particular DCP concentration, the torque increases with rubber content, which results from the predominant crosslinking of the rubber phase. Additionally when the rubber phase is dominant it becomes continuous phase and the crosslinked continuous phase shows high viscosity. Thus when the rubber phase forms the continuous phase the crosslinking is more efficient.

Mechanical properties

Effect of DCP dosage

DCP is capable of crosslinking both phases and there is the chance of graft formation between HDPE and NBR. It was observed that the tensile strength of HDPE was adversely affected upon vulcanization by DCP. This is attributed to the reduction in crystallinity. In the case of NBR, however, a substantial improvement in tensile strength can be observed upon vulcanization, so a significant improvement in mechanical properties can be expected only in rubber-rich blends.

The stress–strain behavior of unvulcanized and dynamically vulcanized H_{70} blend, containing different levels of DCP, is shown in Figure 3. From Figure 3 it is clear that all the H_{70} blends show the stress–strain behavior characteristic of a plastic (i.e., they show very high initial modulus with yielding and necking). It is also clear that with an increase in DCP content corresponding increases in the tensile strength and elongation at break are observed. In unvulcanized H_{70}, the rubber is dispersed as large inclusions in the HDPE matrix because of the high interfacial tension and the poor adhesion between the phases. It is widely accepted that in an immiscible blend the particles of the

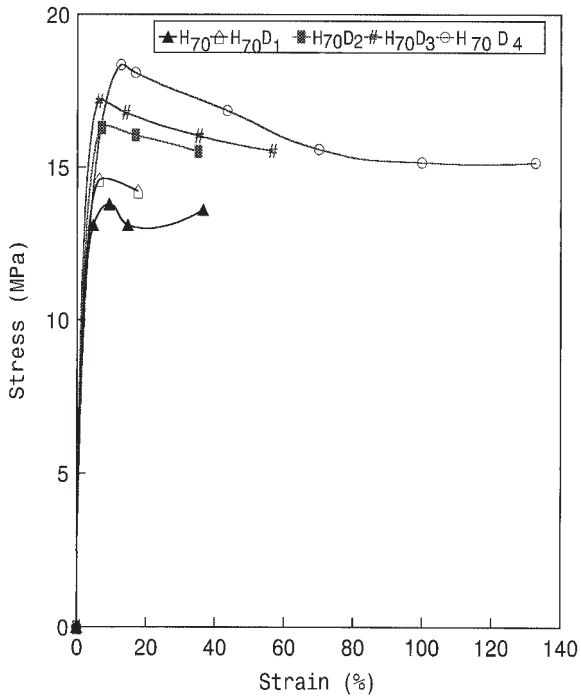

Figure 3 Stress–strain plots of unvulcanized and dynamically vulcanized 70/30 blend of HDPE and NBR containing different levels of DCP.

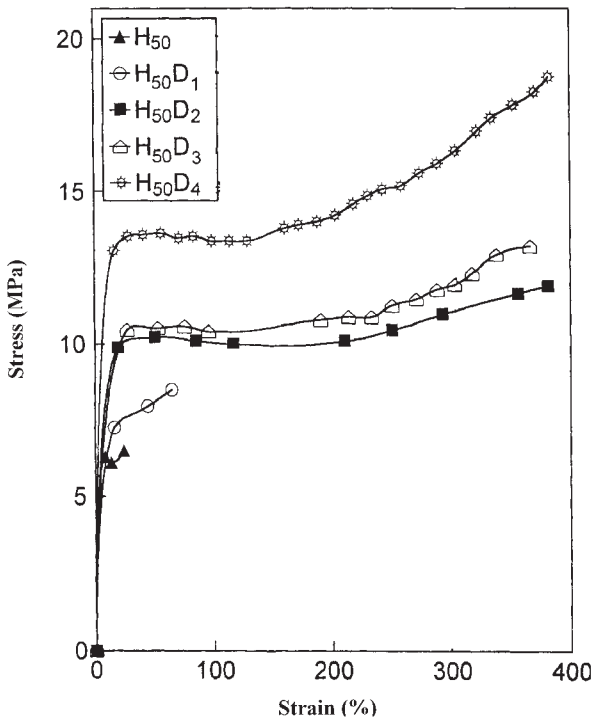

Figure 4 Stress–strain plots of unvulcanized and dynamically vulcanized 50/50 blend of HDPE and NBR containing different levels of DCP.

dispersed phase act as stress- concentrating flaws introducing weak points in the matrix material. As a result an intrinsically tough matrix breaks at a lower stress and at a lower elongation. Thus the comparatively large rubber particles observed in H_{70} act as crack-initiating flaws, resulting in reduced tensile strength and elongation at break. With the addition of DCP, the rubber particles become crosslinked during melt mixing and the morphology is substantially modified. As the percentage of DCP increases, the extent of crosslinking also increases, leading to the formation of fine crosslinked rubber particles in the matrix. Also, morphological stability is imparted by the suppression of coalescence resulting from the decreased diffusional mobility of the crosslinked rubber chains. The crosslinked rubber particles, if attached to the matrix, can withstand greater stress by undergoing increased extent of deformation before failure, thus resulting in increased tensile strength and elongation at break.

The stress–strain curves of unvulcanized and dynamically vulcanized H_{50}, containing different levels of DCP, are shown in Figure 4. The tensile strength of H_{50} is much lower than the theoretically calculated value (18.4 MPa) based on the additivity rule, which is a clear indication of the incompatibility between the phases. Also, the large rubber particles dispersed in the HDPE matrix are ineffective in stress transfer and act as stress-initiating flaws, resulting in reduced tensile strength. A significant change in the morphology is observed upon dynamic vulcanization. The finer and stable morphology of the vulcanized composition contributes toward enhanced tensile strength.

The stress–strain plots of unvulcanized and dynamically vulcanized H_{30} are presented in Figure 5. The unvulcanized H_{30} acts as a weak and soft material. The drastic reduction in the tensile strength of H_{30} may be attributed to the higher proportion of rubber and also to the transition of the rubber phase from the dispersed state to a cocontinuous morphology. However, a substantial increase in tensile strength can be observed in vulcanized blends. On comparing the three blends, H_{70}, H_{50}, and H_{30}, it is seen that the increase in tensile strength with DCP dosage is highest in H_{30}. A 400% increase in tensile strength can be observed in $H_{30}D_4$.

The variations of the ultimate strength with DCP dosage of the blends H_{70}, H_{50}, and H_{30} are shown in Figure 6. In all the blends, the ultimate strength increases with DCP dosage and the increase is substantial in high-rubber blends.

The morphologies of the unvulcanized and dynamically vulcanized H_{70}, H_{50}, and H_{30} are shown in Figure 7(a)–(f). In unvulcanized blends, the rubber exists as large spherical domains in the HDPE matrix until the rubber content is 50% [Fig. 7(a) and (b)]. When the rubber becomes the major phase, a cocontinuous morphology is observed [Fig. 7(c)]. On dynamic vulcanization, the morphology is substantially modified. In all three blends the crosslinked rubber particles exists

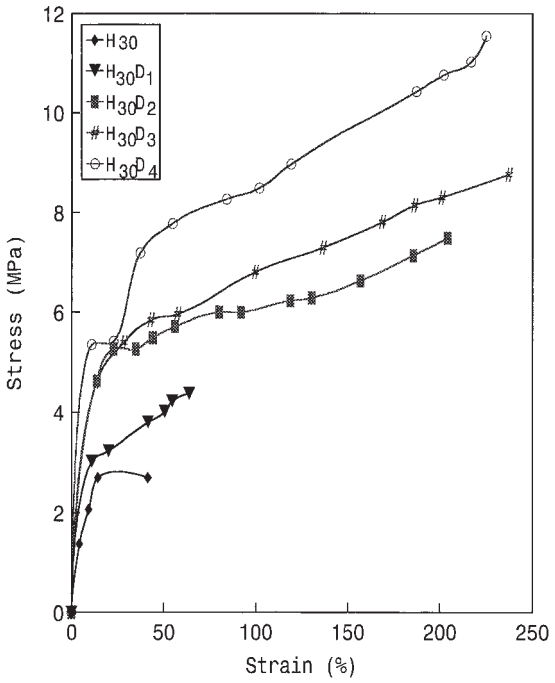

Figure 5 Stress–strain plots of a 30/70 blend of HDPE and NBR indicating the effect of DCP dosage on stress–strain behavior.

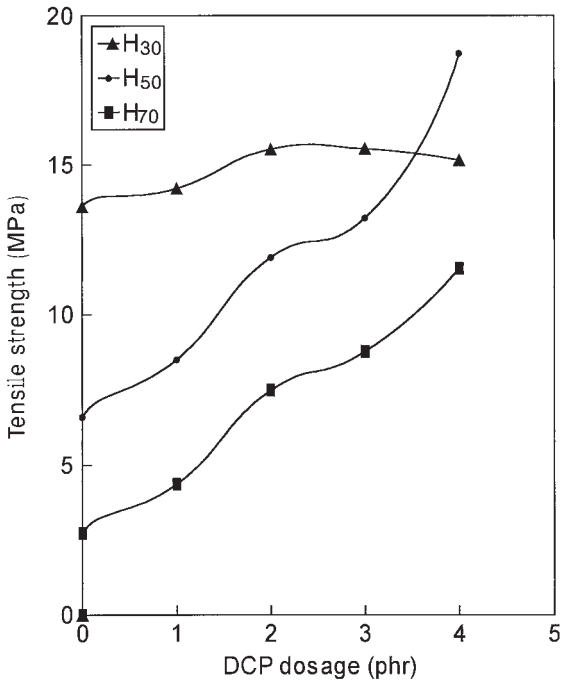

Figure 6 Variation of ultimate strength with DCP dosage of 70/30, 50/50, and 30/70 blends of HDPE and NBR.

as dispersed domains with fine morphology. Also, crosslinking imparts morphological stability by suppressing the tendency toward coalescence.

The crosslink densities of the blends at different levels of DCP were determined by an equilibrium swelling method using toluene as the solvent at 30°C. The variation of V_r (volume fraction of rubber in the solvent swollen sample) values with DCP dosage for the three different blends are presented in Figure 8. In all the blends, V_r values increase with DCP dosage as the resistance to swelling increases, which is a clear indication of the increased extent of crosslinking with DCP content. At any particular DCP level, the V_r value is the highest for H_{70}, followed by H_{50}, and H_{30} shows the lowest value. This is explained by the fact that the plastic phase merely acts as a filler and the solvent uptake is only a result of the rubber phase. Thus H_{70} and H_{30} can be considered as rubber samples with high and low levels of filler (plastic), respectively. As a result, in a high plastic blend the resistance to swelling is high or the solvent uptake is less, thereby resulting in high V_r values.

Variation of yield strength and Young's modulus with crosslink density of H_{70} is presented in Figure 9. From the figure it is clear that the yield strength increases with increasing crosslink density. The Young's modulus, calculated from the initial straight-line portion, increases up to 3 phr DCP. However, at 4 phr DCP the Young's modulus shows a significant reduction. This may be explained by the fact that major structural rearrangement occurs at this level of DCP, which in turn modifies the stress–strain curve and thereby affects the modulus values.

Variation of tensile strength and Young's modulus with crosslink density of dynamically vulcanized H_{30} is presented in Figure 10. The tensile strength increases with increasing crosslink density, increasing 2.5 times from 1 to 4 phr DCP. The significant increase in tensile strength is attributed to the increased extent of crosslinking by DCP in high-rubber blends. However, the Young's modulus values initially show an increase with increasing crosslink density and thereafter a decrease.

The effect of dynamic vulcanization (4 phr DCP) on the tear behavior of H_{70}, H_{50}, and H_{30} are shown in Figure 11. From the figure, it is clear that the dynamic vulcanization significantly improves the tear strength values. The reason given for tensile strength improvement also holds good for tear strength. In an unvulcanized HDPE/NBR blend the dispersed phase acts as a crack-initiating flaw. In a dynamically vulcanized blend, however, the dispersed rubber particles enhance the energy-absorption capacity of the matrix by promoting and controlling the deformation of the matrix. Crazing and shear yielding are the deformation mechanisms. The factors that control the tear strength include the degree of adhesion, degree of crosslinking, and rubber particle size, for example. The particle size and the size distribution have a strong influence on the tear strength. At the optimum size, a large number of small crazes are formed and thereby enhance its ultimate properties. When the rubber particles are uncrosslinked, the molecular entanglements are insufficient to prevent rapid flow and premature failure occurs in response to an applied stress. In crosslinked samples, however, grafts are possible across the interface because the DCP can crosslink both phases. As a result, the rubber particles can elongate to very large tensile strains, giving a crazelike structure.

The variation of tear strength with DCP dosage of the different blends is shown in Figure 12. From the figure it is clear that the tear strength of the blends H_{70} and H_{50} increases with DCP dosage. However, in H_{30}, at 4 phr DCP dosage, the tear strength decreases. This means that excessive crosslinking has occurred in H_{30}. Based on the deformation processes occurring just ahead of the crack tip in rubber-toughened polymers, Yee[29] proposed that certain conditions must be satisfied for maximum toughening. First, the toughening particles should be much smaller than the size of the crack tip and plastic zone. Second, they should debond or cavitate at stresses just below that for failure of the matrix material, thereby relieving triaxial tension and initiating the formation of shear bands. In the present case, the highly crosslinked rubber particles in 4 phr DCP-cured H_{30} will not effectively transfer the stresses to the matrix, thereby resulting in slightly reduced tear strength.

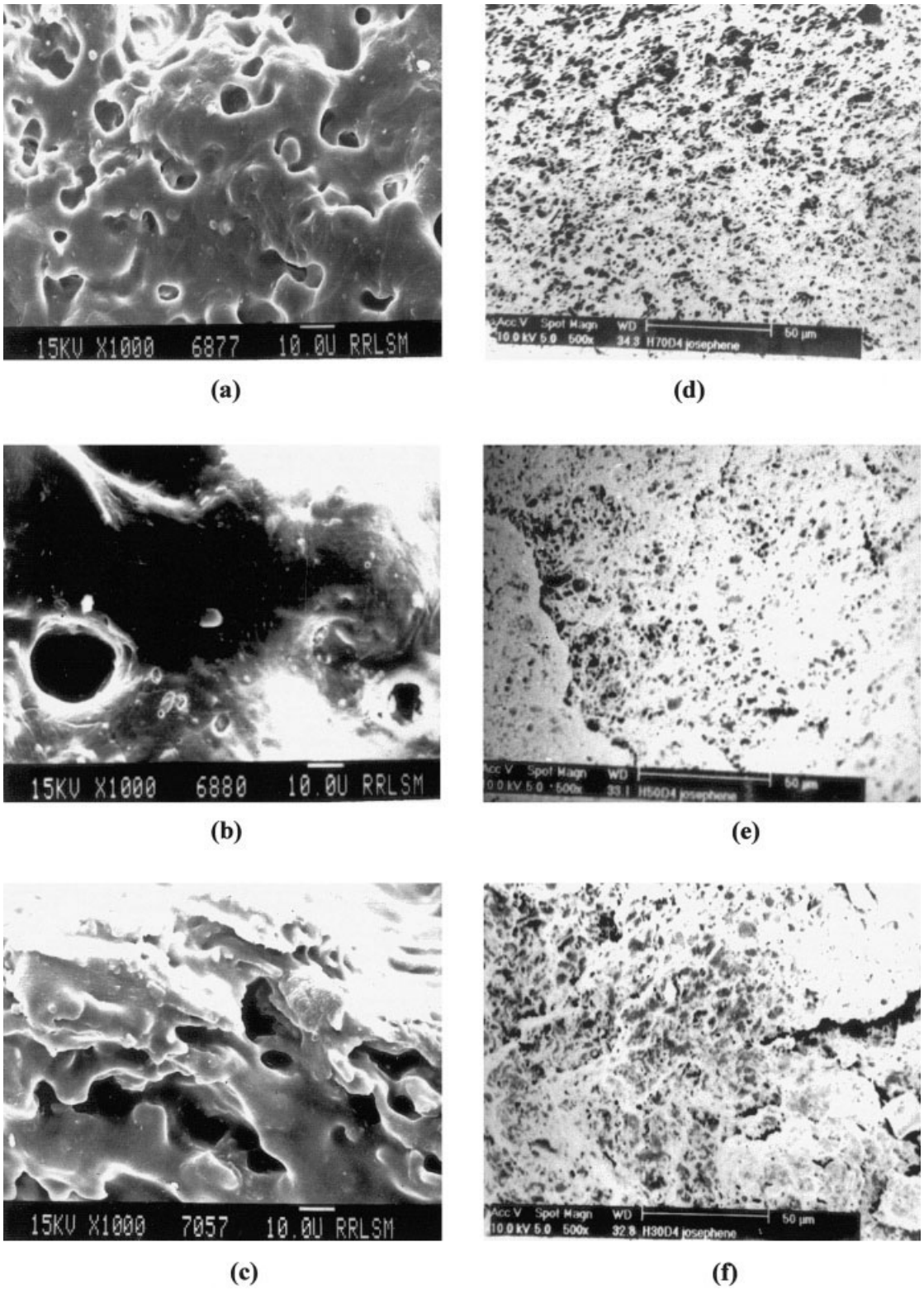

Figure 7 SEM micrographs showing the effect of dynamic vulcanization on the morphologies of blends of HDPE and NBR: (a) H_{70}, (b) H_{50}, (c) H_{30} (×1000); and (d) $H_{70}D_4$, (e) $H_{50}D_4$, (f) $H_{30}D_4$ (×500).

Effect of types of crosslinks

The types of crosslinks on the mechanical properties of the blends are explained using H_{30} as an example. The stress–strain properties of H_{30} vulcanized using sulfur, peroxide, and mixed cure systems are presented in Figure 13. From the figure it is clear that the DCP-cured system acts like vulcanized rubbers; however, the sulfur system seems to be very weak and brittle.

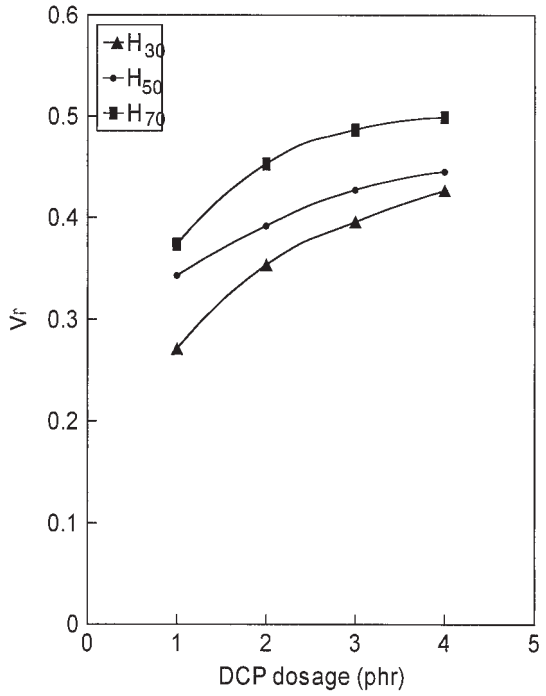

Figure 8 Effect of DCP dosage on the V_r values of different blends of HDPE and NBR.

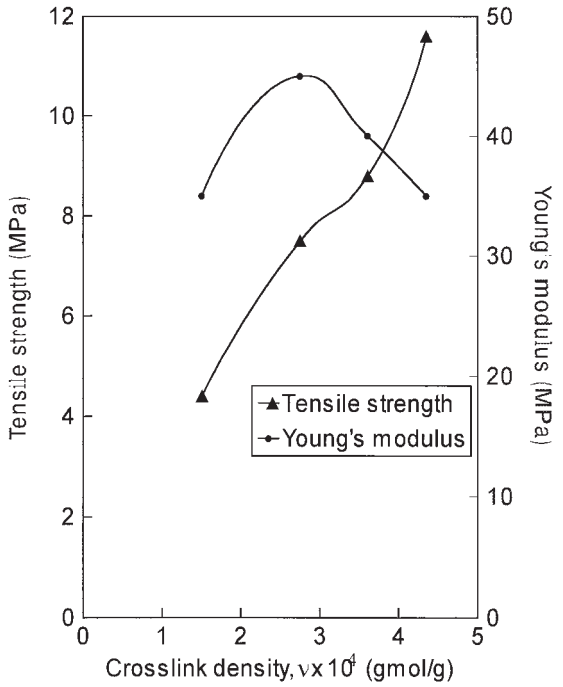

Figure 10 Effect of crosslink density on the tensile strength and Young's modulus of dynamically vulcanized H_{30}.

This may be attributed to the presence of poorly crosslinked large rubber particles present in the sulfur-cured system. The coarse rubber particles act as stress-concentrating flaws, resulting in premature failure. In the peroxide-cured system, the crosslinked rubber particles exert increased torque during mixing and effective particle breakdown occurs. Also, there is chance for graft formation between HDPE and NBR phases. Both of these account for the very good im-

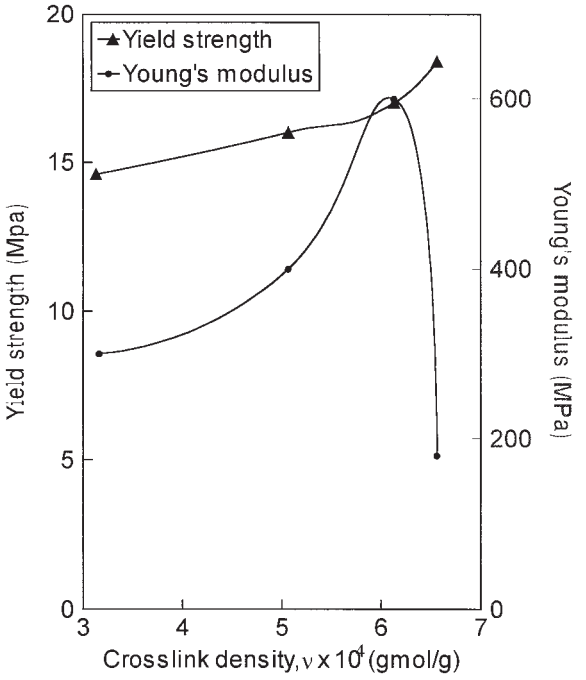

Figure 9 Variation of yield strength and Young's modulus with crosslink density of dynamically vulcanized H_{30}.

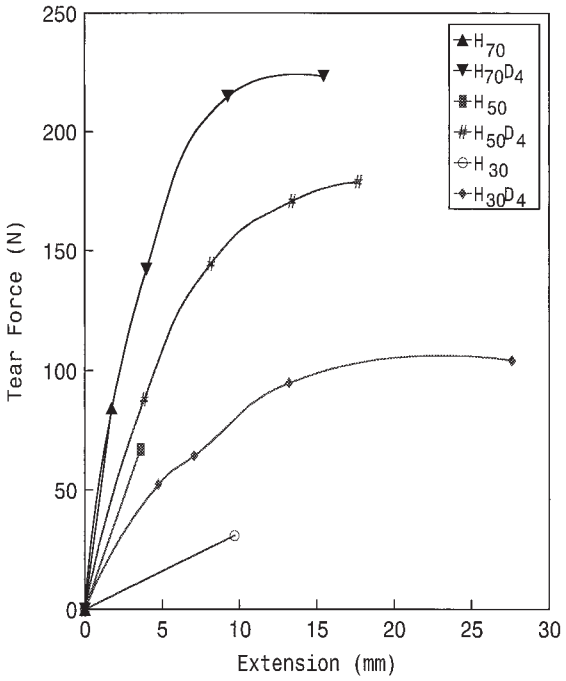

Figure 11 Tear behavior of unvulcanized and dynamically vulcanized 70/30, 50/50, and 30/70 blends of HDPE and NBR.

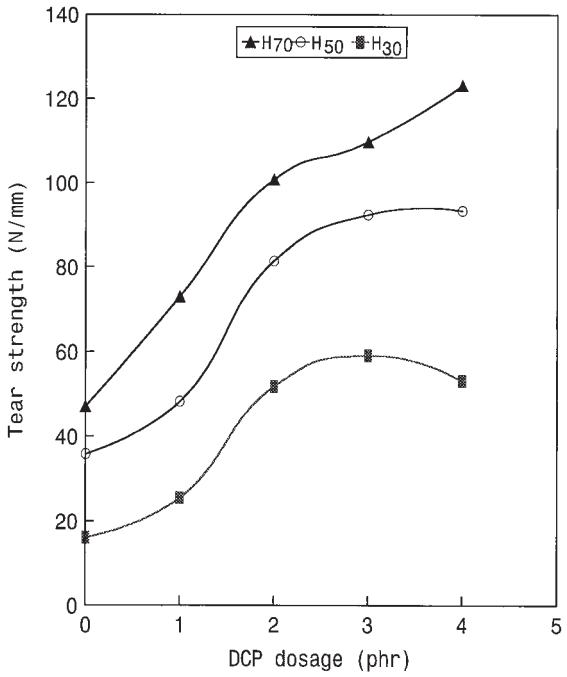

Figure 12 Effect of DCP dosage on tear strength values of different blends of HDPE and NBR.

provement in ultimate properties. The mixed curing system exhibits stress–strain properties intermediate to those of sulfur- and peroxide-cured systems. Usually C–C linkages present in the peroxide-cured system are thermally more stable compared to S–S linkages seen in the sulfur-cured system; thus some of the crosslinks (S–S) will be lost at the time of processing. In the mixed cured system both linkages (C–C and S–S) are possible and thereby have intermediate stability. Thus the morphology, crosslink density, and the type of linkages all account for the differences in the stress–strain properties of blends vulcanized using different curing systems.

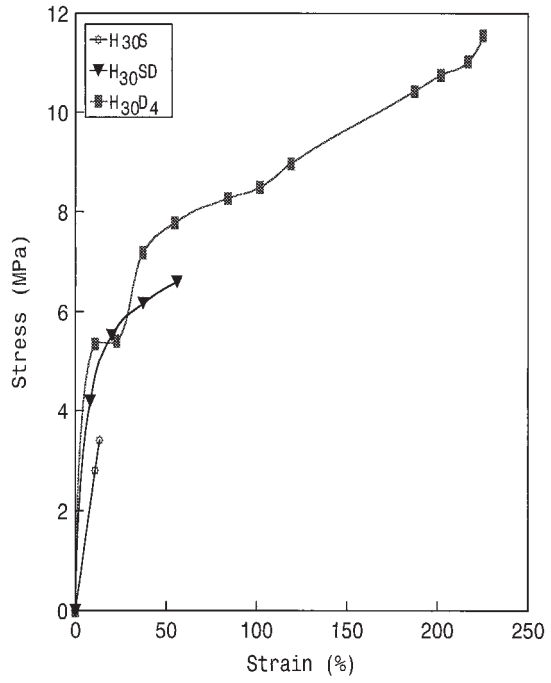

Figure 13 Types of crosslinks on the stress–strain properties of a 30/70 blend of HDPE and NBR.

TABLE I
Effect of Crosslinking System on the Crosslink Density of H_{30}

Crosslinking system	Crosslink density $\nu \times 10^4$ (gmol/g)
Sulfur	1.2583
Mixed (sulfur + DCP)	2.6752
DCP	4.3528

Crosslink densities of H_{30} vulcanized using different curing systems are presented in Table I. It is seen that the crosslink density of the DCP-cured blend is roughly four times that of the sulfur-cured blend. The H_{30} blend, vulcanized using the mixed curing system, exhibits an intermediate crosslink density value. Because crosslink density is one of the major factors controlling the mechanical properties of a vulcanized blend, an increase in mechanical properties can be correlated with the extent of crosslinking.

The effects of type of crosslinking system on the ultimate properties of the blends are presented in Table II. The general trend is the same in all the blends. One can notice that with respect to properties the sulfur system is least favored, followed by mixed and peroxide-cured systems. It can be observed that in the sulfur system, the tear values are lower than those of unvulcanized system, although mixed and peroxide-cured systems show substantial improvement in tear strength. The efficiency of the DCP-cured system can best be explained by the morphological changes. In the sulfur system, the rubber is insufficiently crosslinked and, in fact, at the processing temperature the low viscosity melt of the crosslinking agents just rolls over the high viscosity polymer melt and no proper mixing occurs. As a result insufficient crosslinking occurs. Also because of the lubricating action of the ingredients, the already crosslinked rubber particles cannot exert resistance to rotation, which in turn hinders the breaking up of the rubber into smaller domains. In fact, the large, lightly crosslinked rubber particles aggravate the phase separation and the interface becomes very weak, thus resulting in inferior properties. In the DCP-cured system, the curatives become properly mixed with the polymer and the crosslinked rubber particles exert increased resistance to rotation during mixing. This increased thrust results in breaking up of the crosslinked particles into

TABLE II
Effect of Crosslinking System on the Ultimate Properties of the Blends

Sample code	Properties[a]											
	Tensile strength (N/mm^2)				Tear strength (N/mm)				Elongation at break (%)			
	U	S	SD	D	U	S	SD	D	U	S	SD	D
H_{70}	13.6	13.3	17.7	15.2	47.1	31.7	74.8	126.1	36	5	11	132
H_{50}	6.6	7.2	11.8	18.8	35.9	31.2	50	93.4	24	15	38	382
H_{30}	2.7	3.4	6.6	11.6	16.1	13.6	30.4	53.1	41	13	56	225

[a] U, unvulcanized; S, sulfur cured; SD, mixed cured; D, DCP cured.

fine domains. The small size of the particles and the uniformity in particle size distribution both account for the enhancement in tear strength values of DCP-cured systems.

In the mixed cured system, the properties are intermediate. Here also crosslinking and breaking up of the crosslinked particles take place but to a lesser extent compared to that in the DCP-cured system.

The final torque values of unvulcanized and dynamically vulcanized blends crosslinked by different curing agents are presented in Figure 14. It is seen that sulfur curing results only in a slight increase in the torque values in all the blends. In fact the extent of crosslinking is reflected in the torque values. The low torque values indicate that the sulfur systems are inefficiently crosslinked. The high torque values of DCP-cured blends reveal that it is the most efficient vulcanization system and the mixed curing system has intermediate efficiency.

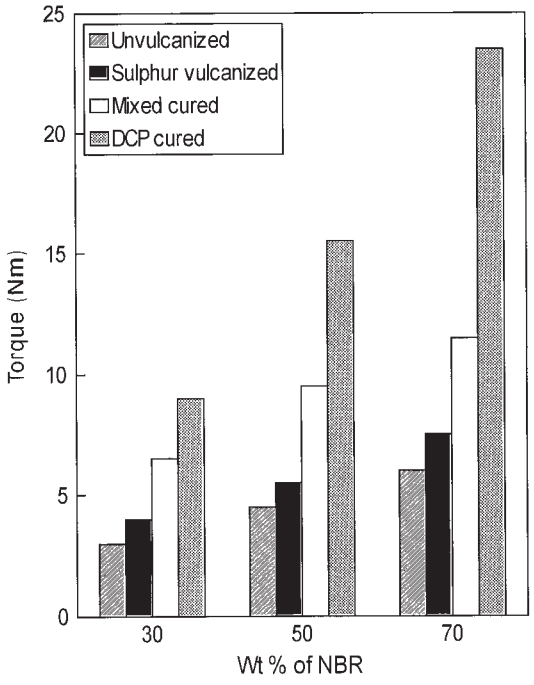

Figure 14 Bar graph indicating the effect of various crosslinking systems on the final torque values of 70/30, 50/50, and 30/70 blends of HDPE and NBR.

The morphology changes, associated with different curing systems, are illustrated by taking H_{50} as an example. The morphologies of H_{50}, $H_{50}S$, $H_{50}SD$, and $H_{50}D_4$ are presented in Figure 15(a)–(d). In H_{50} the rubber is dispersed as large domains in the HDPE matrix. The high interfacial tension and poor adhesion between HDPE and NBR result in aggressive phase separation. During melt mixing fine morphology is obtained because of high shearing action, but on sheeting or under service conditions particle coalescence can occur and the coalesced particles are rejected from the matrix, resulting in poorly bonded large rubber particles. However, in vulcanized samples [Fig. 15(b)–(d)] effective particle breakdown occurs and stabilization of morphology occurs because of the absence of the coalescence process. Also, it is clear that the size of the dispersed domains decreases in the order $H_{50}S > H_{50}SD > H_{50}D_4$. The number-average particle sizes for H_{50}, $H_{50}S$, $H_{50}SD$, and $H_{50}D$ are 14.28, 3.49, 2.36, and 1.91 μm, respectively. The particle size was measured by an image analysis technique that considers a large number of particles.

The tensile fractographs of H_{70}, $H_{70}D_1$, $H_{70}D_2$, and $H_{70}D_3$ are shown in Figure 16(a)–(d). In unvulcanized H_{70} [Fig. 16(a)] premature failure occurs because of the poor bonding between the rubber and plastic. However, dynamic vulcanization improves the rubber–plastic adhesion by graft formation. The significant deformation of the matrix, observed in dynamically vulcanized blends [Fig. 16(b)–(d)], is an indication of improved adhesion. Also, it is evident that the matrix deformation increases with increasing DCP concentration.

Effect of filler incorporation

Types of filler and filler loading on stress–strain properties. The stress–strain properties of dynamically vulcanized H_{30} and H_{30}, containing 30 phr of different fillers such as carbon black, cork, silica, and treated silica, are shown in Figure 17. It is clear from the figure that the tensile strength is enhanced by the incorporation of carbon black, silica, and treated silica. However, cork filler results in deterioration in mechanical properties. The reinforcement by a filler is dependent

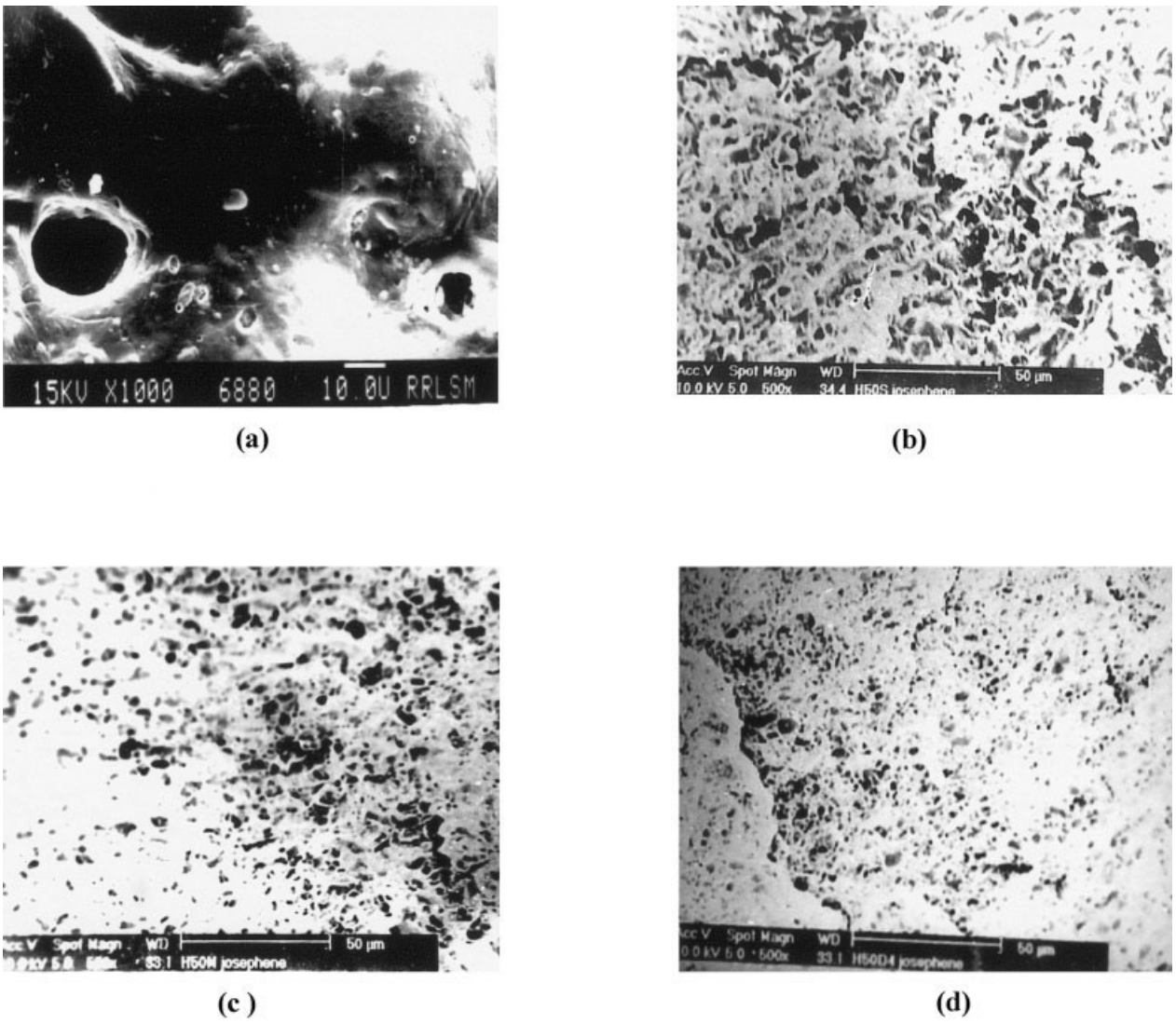

Figure 15 Types of crosslinks on the morphologies of a 50/50 blend of HDPE and NBR: (a) H_{50}, (b) $H_{50}S$, (c) $H_{50}SD$, and (d)$H_{50}D_4$.

on so many factors such as particle size, size distribution, structure, surface characteristics, and filler–matrix adhesion, for example. Fillers of sufficiently small particle size will all give about the same order of magnitude in reinforcement if there are no great differences in particle shape. Thus carbon black (29 nm) and silica (20 nm) give almost the same extent of reinforcement and cork filler results in inferior properties because of its comparatively large size.

The effect of carbon black loading on the stress–strain properties of H_{30} is presented in Figure 18. From the figure, it is clear that the tensile strength shows a marginal increase with increasing filler loading, which is an indication of the reinforcement by the filler. The elongation at break is scarcely affected by filler incorporation.

The effect of filler loading on the ultimate strength of $H_{30}D_4$ containing different fillers is presented in Figure 19. From the figure it is clear that, except for cork filler, there is an increase in tensile strength with filler loading. Also, treatment of silica filler with silane coupling agent results in improvement in ultimate strength in all cases except for 30 phr filler. The enhancement in properties may be explained by the improved interfacial adhesion between the filler and the rubber. Usually the coupling agents have an organic and an inorganic part. The coupling agent modifies the interface between the rubber and the filler and enhances the bonding between the filler and the rubber. Thus the interfacial adhesion is enhanced, which is reflected in increased tensile strength.

In the case of cork filler, a reverse trend is observed (i.e., the tensile strength decreases with filler loading). This may be attributable to the insufficient wetting of the filler by the rubber and may also be attributable to the large size of the filler compared to that of C-black and silica.

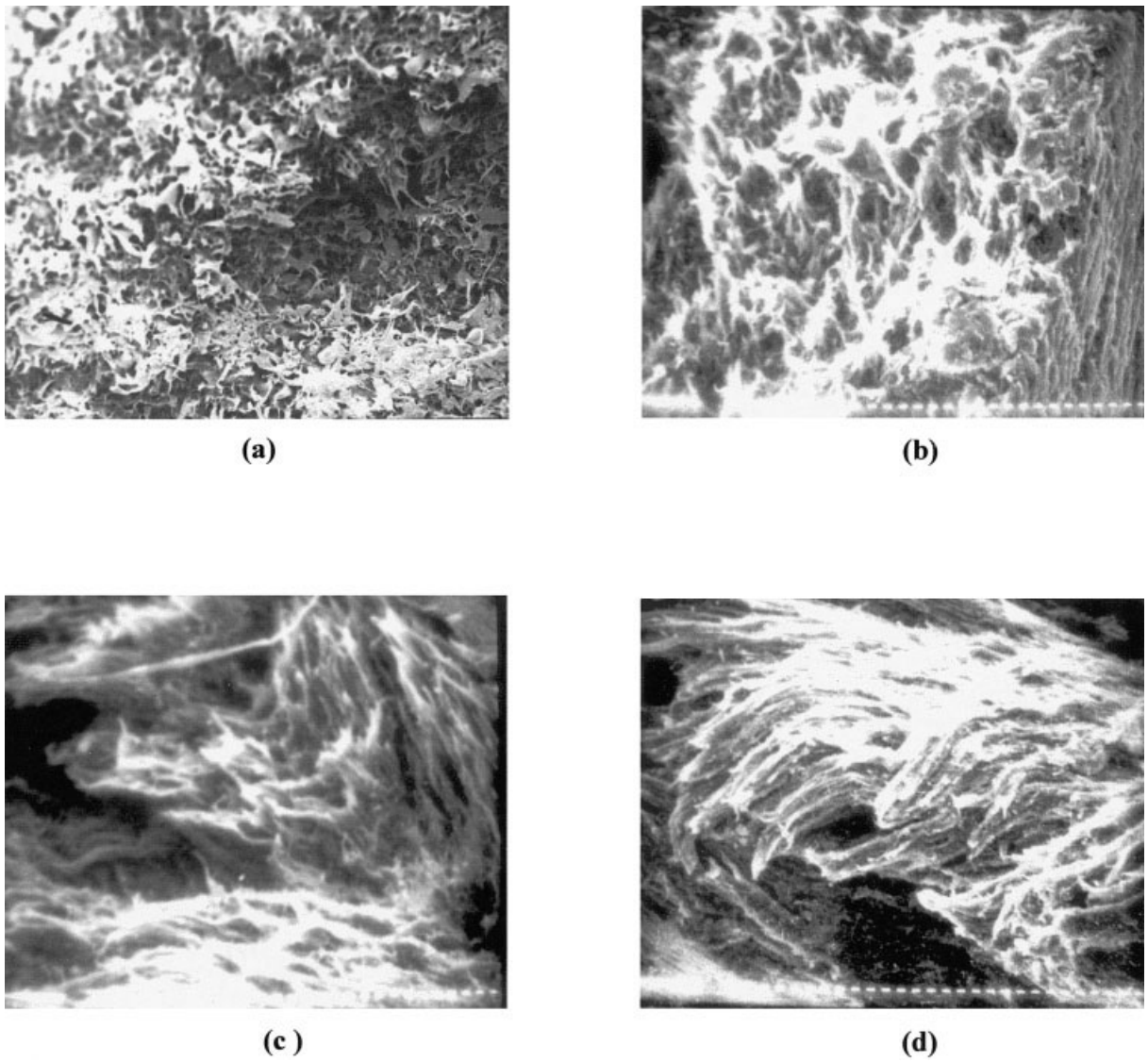

Figure 16 Tensile fractographs showing the effect of DCP dosage on the deformation pattern of H_{70} blends (×200): (a) H_{70}, (b) $H_{70}D_1$, (c) $H_{70}D_2$, and (d) $H_{70}D_3$.

Variation of Young's modulus with filler loading of dynamically vulcanized H_{30} is presented in Figure 20. A significant increase in Young's modulus over the unfilled one is observed in all the fillers, even at 10 phr loading. Even though cork-filled samples have inferior tensile strength, the Young's modulus is high. This may be attributable to the comparatively high modulus of the filler. This high modulus contributes toward good initial load-bearing capacity, but in tensile strength measurement the interfacial bonding also enters the picture. Thus in cork-filled samples a high Young's modulus is observed, even though its tensile strength is affected by filler incorporation. In the other two fillers (carbon black and treated silica) the Young's modulus values increase but not in proportion to the weight fraction of the filler.

Effect of filler on tear properties

The effect of C-black, cork, silica, and treated silica on the tear force–extension behavior of $H_{30}D_4$ is presented in Figure 21. From the figure it is clear that an enhancement in property is obtained only with silica filler. As observed in other properties, such as tensile strength and elongation at break, cork filler results in a considerable decrease in tear strength. Another important difference is that, unlike tensile strength and elongation at break, the tear strength of 30 phr C-black–loaded H_{30} is less than that of unfilled one. This can be explained on the basis of the deformation pattern during tearing. The excessive crosslinking and the high loading of the filler make the matrix somewhat rigid. In tear testing the predominant ways of energy absorption are crazing and shear yielding. For proper

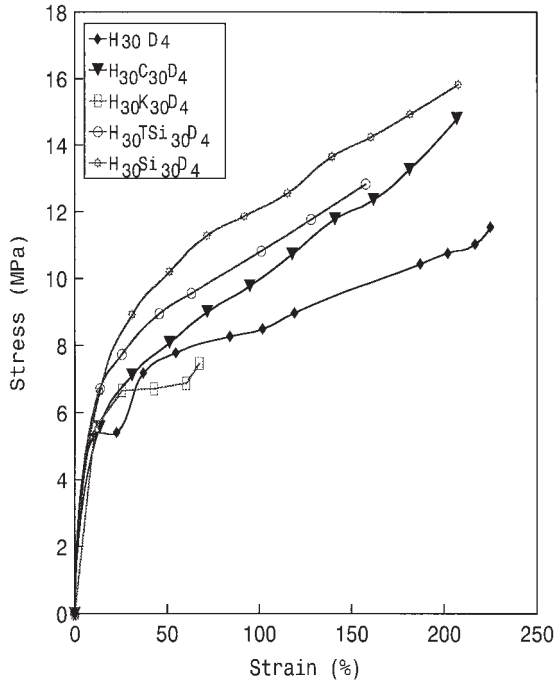

Figure 17 Stress–strain properties of dynamically vulcanized unfilled and 30 phr filled 30/70 blend of HDPE and NBR.

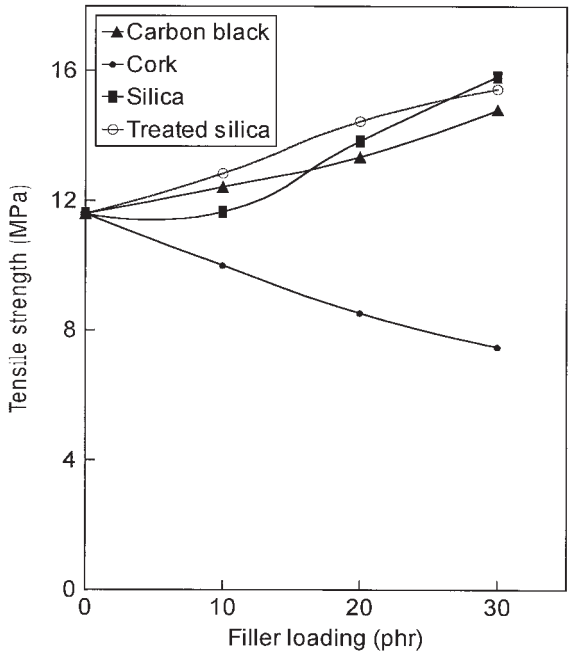

Figure 19 Effect of filler loading on the ultimate strength of dynamically vulcanized 30/70 blend of HDPE and NBR.

energy absorption a balance between filler loading and crosslink density should be maintained. The use of fine-particle silica at lower loadings has been reported to improve the physical properties of thermoplastic elastomer blends.[30] At higher filler loadings the material may undergo a brittle type of failure, resulting in reduced tear strength. This is made clear when we look at the effect of carbon black loading on the tear behavior of the H_{30} blend.

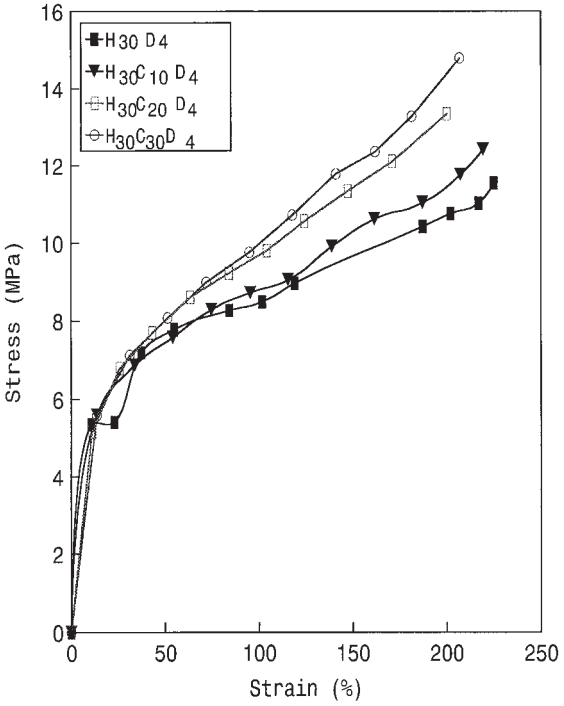

Figure 18 Effect of carbon black loading on the stress–strain properties of dynamically vulcanized 30/70 blend of HDPE and NBR.

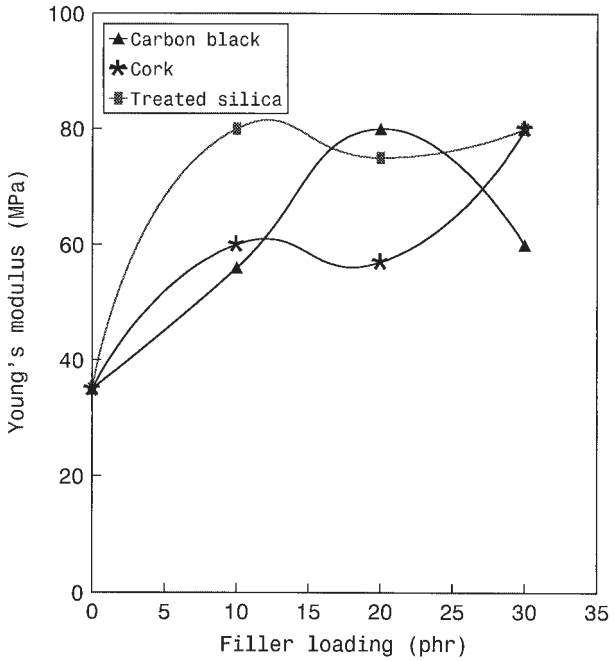

Figure 20 Effect of filler loading on the Young's modulus values of dynamically vulcanized H_{30}.

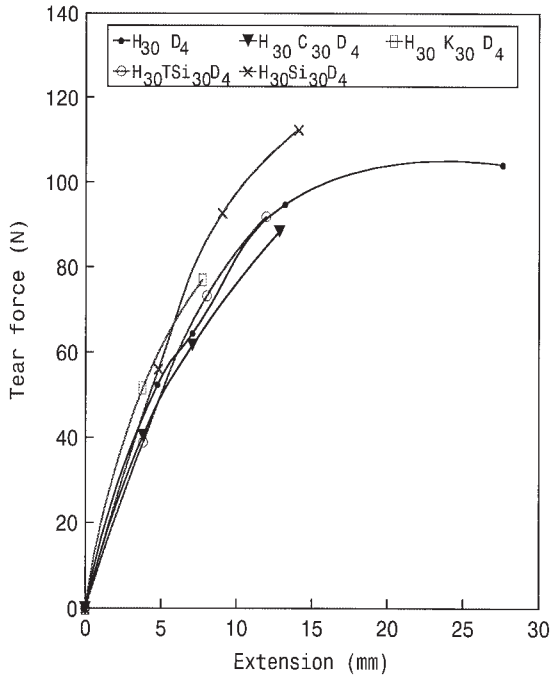

Figure 21 Force–extension behavior of unfilled and filled dynamically vulcanized 30/70 blend of HDPE and NBR.

The effect of C-black loading on the tearing pattern of $H_{30}D_4$ is presented in Figure 22. A substantial increase in tear strength is observed with only 10 phr filler, although the strength decreases on adding further quantity of filler. This may be a result of the increased filler–filler contact rather than the filler–rubber contact, in highly filled blends.

The tear fractographs of H_{50}, $H_{50}D_4$, and $H_{50}K_{30}D_4$ are presented in Figure 23(a)–(c). Unvulcanized H_{50} [Fig. 23(a)] acts as a weak and brittle material because of the incompatibility. When a tear force is applied, failure occurs without any matrix deformation, but in $H_{50}D_4$ [Fig. 23(b)] multiple fracture paths can be seen. This is explained by the fact that in dynamically vulcanized H_{50} a large number of small crosslinked rubber particles are present that enhance the rubber plastic adhesion. Also, these particles promote and control the tearing behavior by transferring the stresses to the matrix. In $H_{50}K_{30}D_4$ [Fig. 23(c)], large debonded domains can be seen that aggravate the incompatibility problem. These large debonded domains cannot hinder a propagating crack and premature failure occurs.

Theoretical modeling

In a two-phase system, theoretical models could correctly predict the way by which the phases interact (respond) toward a particular deformation. In an incompatible blend, some anomaly may be seen in the property–composition curve. We could account for this by carrying out model calculations. The best-fit model curve to that of the experimental curve tells us about the way in which the blend components respond toward an applied stress. The various models analyzed include parallel, series, Halpin–Tsai,[31] Coran's,[32] Takayanagi,[33,34] Kerner,[35] and Kunori[36] models.

According to parallel combination, the property of the blend M is given by

$$M = M_1\phi_1 + M_2\phi_2 \tag{5}$$

where ϕ_1 and ϕ_2 are the volume fractions of the continuous and dispersed phase, respectively. M_1 and M_2 are the properties of phases 1 and 2. The equation for the series combination of the components is represented as

$$\frac{1}{M} = \frac{\phi_1}{M_1} + \frac{\phi_2}{M_2} \tag{6}$$

Subscripts 1 and 2 have the same significance as in eq. (1).

Halpin and Tsai[31] developed equations to cover the complete range of moduli from the lowest lower bound to the highest upper bound.

The Halpin–Tsai equations are

$$\frac{M_1}{M} = \frac{1 + A_iB_i\phi_2}{1 - B_i\phi_2} \tag{7}$$

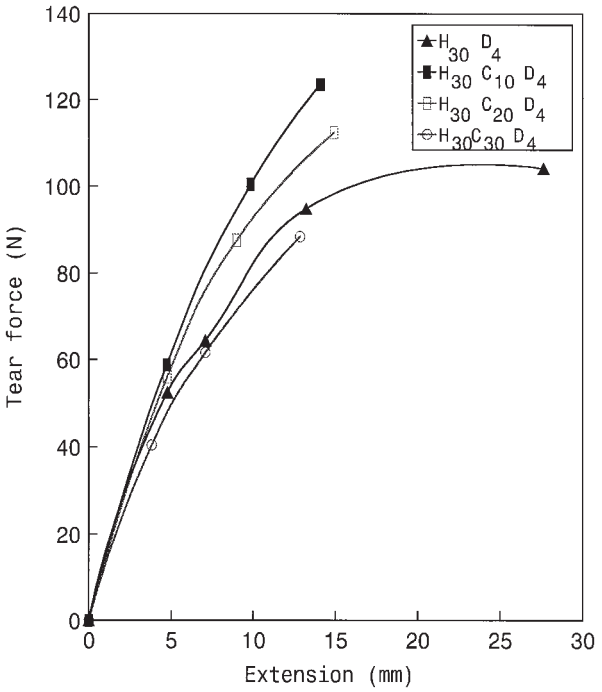

Figure 22 Effect of carbon black loading on the tearing behavior of dynamically vulcanized 30/70 blend of HDPE and NBR.

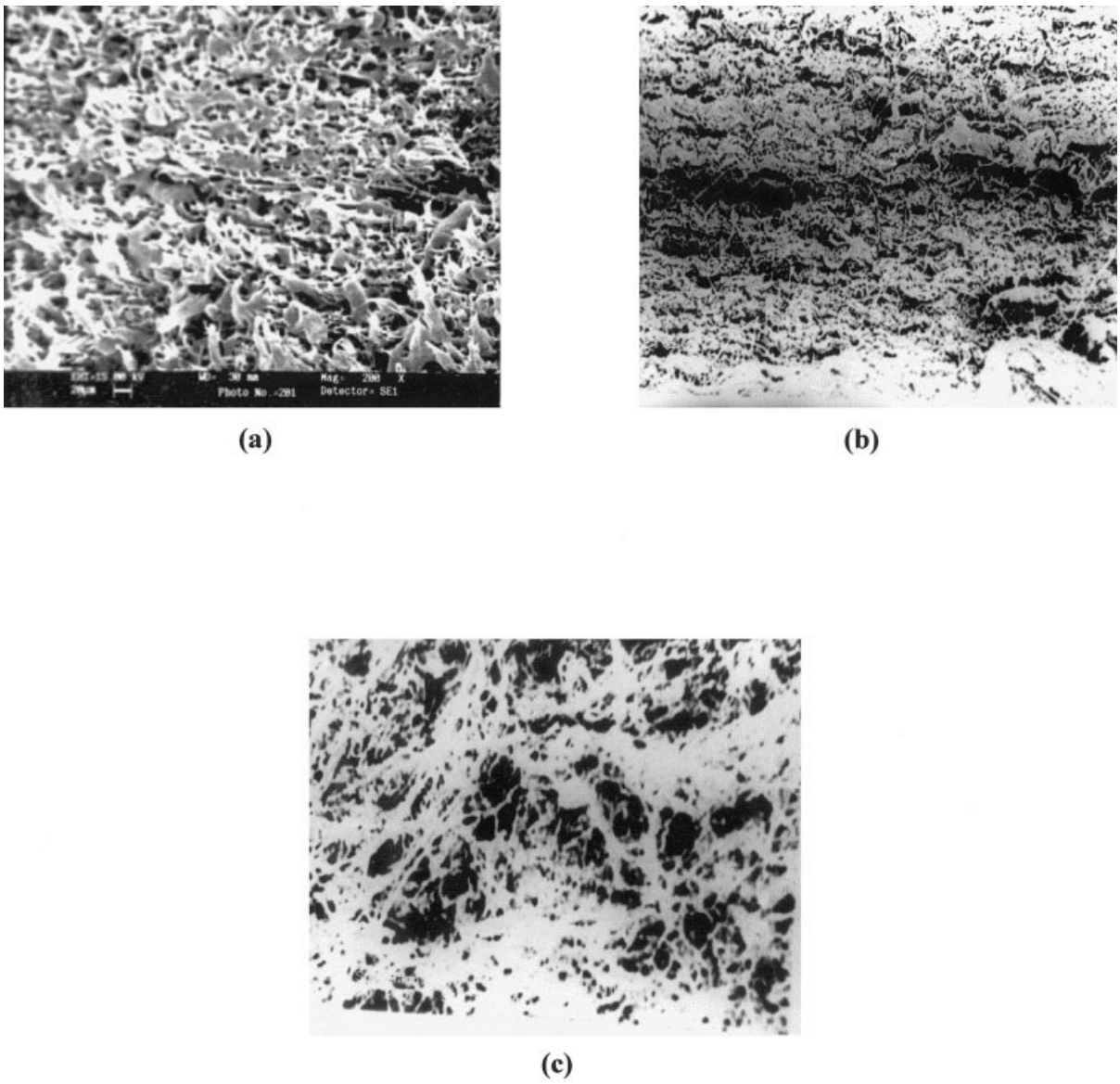

Figure 23 Tear fractographs of 50/50 blend of HDPE and NBR (×200): (a) H_{50}, (b) $H_{50}D_4$, and (c) $H_{50}K_{30}D_4$.

and

$$B_i = \frac{M_1/M_2 - 1}{M_1/M_2 + A_i} \tag{8}$$

Subscripts 1 and 2 represent continuous and dispersed phase. A_i is defined by the morphology of the system. For elastomer domains dispersed in a hard continuous matrix $A_i = 0.66$.

The equations for Coran's model[32] are

$$M = f(M_U - M_L) + M_L \tag{9}$$

where f is a function of phase morphology given by

$$f = V_H{}^n(nV_S + 1) \tag{10}$$

and n contains aspects of phase morphology.

V_H and V_S are the volume fractions of the hard and soft phases, respectively.

According to the Takayanagi model[33,34]

$$M = (1 - \lambda)M_1 + \lambda[(1 - \phi_2)/M_1 + \phi_2/M_2]^{-1} \tag{11}$$

where M_1 is the property of the matrix phase, M_2 is the property of the dispersed phase, and $\phi_2\lambda$ is the volume fraction of the dispersed phase and is related to the degree of series–parallel coupling. The degree of parallel coupling of the model can be expressed by

$$\%\ \text{Parallel} = [\phi_2(1 - \lambda)/(1 - \phi_2\lambda)] \times 100 \tag{12}$$

In Kerner[35] model a new factor, Poisson's ratio, enters the picture. The equation for this model is

$$E_b = E_m\left[\frac{\phi_d E_d/[(7-5\upsilon_m)E_m + (8-10\upsilon_m)E_d] + \phi_m/15(1-\upsilon_m)}{\phi_d E_m/[(7-5\upsilon_m)E_m + (8-10\upsilon_m)E_d] + \phi_m/15(1-\upsilon_m)}\right] \quad (13)$$

where E_b is the blend property, υ_m is Poisson's ratio, and ϕ is the volume fraction. The subscripts m, d, and b stand for the matrix, dispersed phase, and blend, respectively.

Kunori and Geil[36] developed a model to account for the tensile failure of a blend arising from a lack of adhesion between the blend components. When there is no adhesive force between the blend components, the tensile strength of the blends

$$\sigma_b = \sigma_m(1 - A_d) \quad (14)$$

where σ_b and σ_m are the tensile strength of the blend and the matrix, respectively, and A_d represents the area occupied by the dispersed phase in transverse cross section. Kunori and Geil[36] assumed that when a strong adhesive force exists between the blend components, the dispersed phase will contribute to the strength of the blend and therefore the parallel model may be modified as

$$\sigma_b = \sigma_m(1 - A_d) + \sigma_d A_d \quad (15)$$

If the force propagates mainly through the interface the above equation may be written as

$$\sigma_b = \sigma_m(1 - \phi_d^{2/3}) + \sigma_d\phi_d^{2/3} \quad (16)$$

and if the force propagates through the matrix, then the equation becomes

$$\sigma_b = \sigma_m(1 - \phi_d) + \sigma_d\phi_d \quad (17)$$

which is same as parallel model.

For filled systems, the simplest equation for the reinforcement or the increase in rigidity attributed to a filler is given by the Einstein equation. This equation is valid only at low concentrations of filler, when there is perfect adhesion between the phases and can be represented as

$$G = G_1(1 + 2.5\phi) \quad (18)$$

where G is the modulus of the filled system, G_1 is the modulus of the unfilled system, and ϕ is the volume fraction of the filler. Einstein's equation implies that the stiffening or reinforcing action of a filler is independent of the size of the filler particles. The equation shows that the volume occupied by the filler is independent of the size of the filler particles and the volume occupied by the filler, rather than its weight, is the important variable. The equation also assumes that the filler is considerably more rigid than that of the matrix.

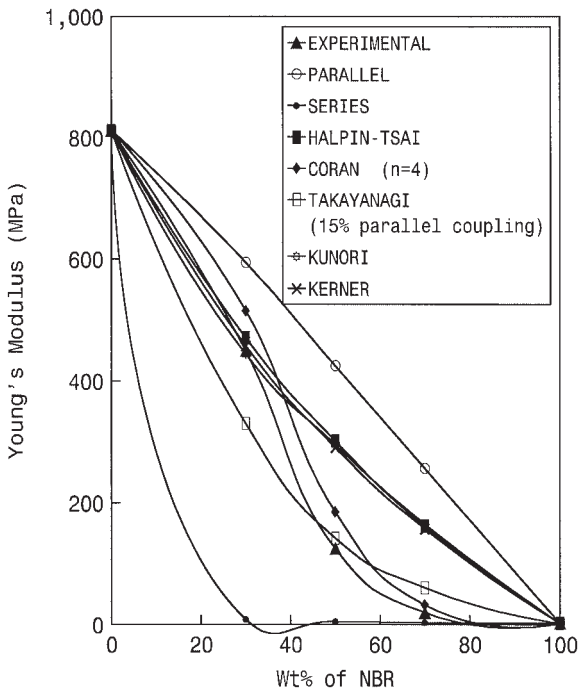

Figure 24 Various theoretical models for the variation of Young's modulus with weight percentage of NBR for unfilled and unvulcanized blends of HDPE and NBR.

An extension of Einstein's theory, originally developed to explain rubber reinforcement, is ascribed to Guth[37] and Smallwood.[38] Their equation for the increase in modulus arising from a rigid spherical filler is

$$G = G_1(1 + 2.5\phi + 1.41\phi^2) \quad (19)$$

where each parameter has the same significance as that of the previous equation.

The curves resulting from different models and that of the experimental data for the variation of Young's modulus with weight percentage of NBR of unvulcanized blends are shown in Figure 24. From the figure it is clear that the Takayanagi model, with 15% parallel coupling, gives the best-fit curve. The parallel and series models show extreme deviations because in an incompatible blend, like HDPE and NBR, uniform stress distribution is virtually impossible. Also, in such blends premature failure may occur because of the stress concentration at the interface.

The different model curves and experimental curve for the variation of Young's modulus with weight percentage of NBR of dynamically vulcanized (4 phr DCP) blends are presented in Figure 25. The series model is the lowest bound and the parallel model is the upper bound over the entire composition range.

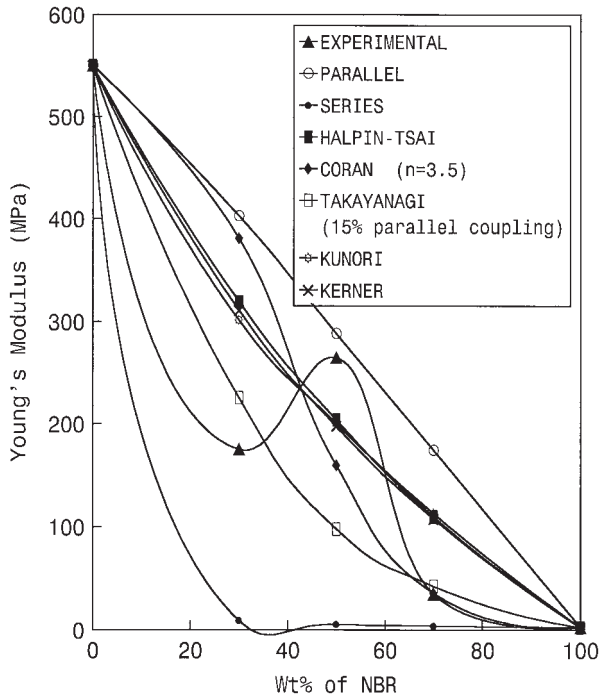

Figure 25 Various theoretical models for the variation of Young's modulus with weight percentage of NBR for dynamically vulcanized blends of HDPE and NBR.

Coran's model shows positive and negative deviations from the experimental values. Out of the various models analyzed, the Takayanagi model gives the best-fit curve over the entire composition range.

The experimental and theoretical variations of Young's modulus with filler loading of dynamically vulcanized H_{30} are presented in Figure 26. The experimental values are higher than those of the theoretical models studied.

CONCLUSIONS

Dynamic vulcanization of HDPE/NBR blends results in an increase in the mixing torque values as a consequence of the crosslinking of the dispersed domains. Out of the three vulcanization systems analyzed, the increase in torque was highest in DCP-cured blends, which is explained by the fact that DCP is capable of crosslinking both phases. The increase in torque with DCP dosage was substantial in high-rubber blends. Mechanical properties indicated a significant enhancement with DCP dosage. Again, the increase was more in rubber-rich blends, attributed to the increase in the extent of crosslinking. The nature and types of crosslinks also have a significant effect on the mechanical properties. The peroxide-cured system is excellent, followed by the mixed cured system, and the sulfur system showed the least improvement. Significant morphology transformation occurred as a result of dynamic vulcanization. In the unvulcanized blend, rubber exists as large particles, thus resulting in inferior properties. However, the rubber particle size decreases with the efficiency of the crosslinking system and its weight percentage. Thus in the present study the 4 phr DCP-cured system resulted in a substantial number of fine rubber particles; however, in the sulfur-cured system the rubber particles are comparatively larger. The particle size of the mixed cured system was between that of sulfur and the DCP-cured system. The fractured surface analysis indicated that premature failure occurs because the interface is weak in unvulcanized blends. On the other hand, in dynamically vulcanized (especially DCP-cured) blends, no such debonding occurs. In fact in such blends yielding of the matrix can be observed. Thus effective stress transfer could occur in dynamically vulcanized blends containing small and uniformly distributed crosslinked rubber particles. Filler incorporation revealed that the reinforcement results only in high-rubber blends. Thus carbon black, silica, and treated silica could marginally improve the mechanical properties of the 30/70 blend of HDPE and NBR. Variation of mechanical properties with filler loading suggested that within the limits of study, the tensile strength increased with filler loading, although the tear strength was adversely affected. However, an increase in tear strength can be observed at 10 phr of treated silica. Treatment of silica with silane coupling agent resulted in a marginal improvement in properties, which may be explained by the improved interfacial bonding between the polymer and the filler. Theoretical modeling sug-

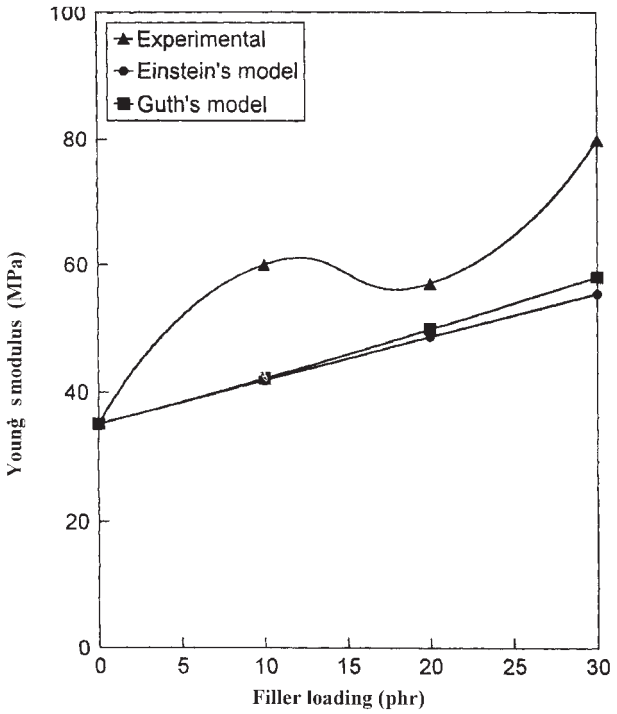

Figure 26 Theoretical models for the variation of Young's modulus with filler loading of dynamically vulcanized H_{30}.

gested that the Takayanagi model, with 15% parallel coupling, relates well to the experimental curves in both unvulcanized and dynamically vulcanized blends. In the case of a filled system the experimental curve lay above the theoretical curves.

References

1. Xanthos, M.; Dagli, S. S. Polym Eng Sci 1991,31, 929.
2. Brown, S. B. in Reactive Extrusion, Principles and Practice; Xanthos, M., Ed.; Hanser: New York, 1992; p 75–199.
3. Liu, N. C.; Baker, W. E. Adv Polym Technol 1992, 11, 249.
4. Bonner, J. G.; Hope, P. S. in Polymer Blends and Alloys; Folkes, M. J.; Hope, P. S., Eds.; Blackie: Glasgow, UK, 1993; p 46–74.
5. Majumdar, B.; Paul, D. R. in Polymer Blends; Paul, D. R.; Bucknall, C. B., Eds.; Wiley: New York, 2000; Vol. 1, Chapter 17.
6. Koning, C.; Duin, M. V.; Pagnoullie, C.; Jerome, R. Prog Polym Sci 1998, 23, 707.
7. Datta, S.; Dharmarajan, N.; Ver Strate, G.; Ban, L. in New Advances in Polyolefins; Chung, T. C., Ed.; Plenum: New York, 1993; p 197–207.
8. Datta, S.; Dharmarajan, N.; Ver Strate, G.; Ban, L. Polym Eng Sci 1993, 33, 721.
9. England, W. P.; Stoddard, G. J.; Scobbo, J. J. U.S. Pat. 5,310,795 (1994).
10. Kitayama, N.; Keskkula, H.; Paul, D. R. Polymer 2001, 42, 3751.
11. Kim, K. J.; Jeong, W. Y. Polymer 2001, 42, 4423.
12. Zhang, J.; He, J. S. Polymer 2002, 43, 1437.
13. Castellano, M.; Nebbia, D.; Turturro, A.; Valenti, B.; Costa, G.; Falqui, L. Macromol Chem Phys 2002, 203, 1614.
14. Tedesco, A.; Krey, P. F.; Barbosa, R. V.; Mauler, R. S. Polym Int 2002, 51, 105.
15. Okada, O.; Keskkula, H.; Paul, D. R. Polymer 2001, 42, 8715.
16. Chang, F. C.; Hwu, Y. C. Polym Eng Sci 1991, 31, 1509.
17. Chen, C. C.; Fontan, E.; Min, K.; White, J. L. Polym Eng Sci 1988, 28, 69.
18. Coran, A. Y.; Patel, R. Rubber Chem Technol 1980, 53, 141.
19. Radusch, H. J.; Lammer, E.; Lupke, T.; Haussler, L.; Sandring, M. Kautsch Gummi Kunstst 1991, 44, 1125.
20. Olivier, E. J. U.S. Pat. 5,003,003, 1991.
21. Moffett, A. J.; Dekkers, M. E. J. Polym Eng Sci 1992, 32, 1.
22. Coran, A. Y.; Patel, R. Rubber Chem Technol 1983, 56, 1045.
23. George, J.; Ramamurthy, R.; Varughese, K. T.; Thomas, S. J Polym Sci Part B: Polym Phys 2000, 38, 1104.
24. Khinnawar, R. S.; Aminabhavi, T. M. J Appl Polym Sci 1991, 42, 2321.
25. Fedors, R. F. Polymer 1979, 20, 1087.
26. Al Malika, S.; Amir, E. J. J Nat Rubber Res 1986, 1, 104.
27. Chodaok, I.; Lazar, M. Angew Makromol Chem 1982, 106, 153.
28. Borsig, F.; Fieldlerova, A.; Lazar, M. J Macromol Sci Chem A 1981, 16, 513.
29. Yee, A. F. in Proceedings of the 3rd European Symposium on Polymer Blends, Cambridge, UK, July 1990.
30. Ramos, L. F.; Valle, D.; Ramirez, R. R. Rubber Chem Technol 1982, 55, 1328.
31. Nielson, L. E. Rheol Acta 1974, 13, 86.
32. Coran, A. Y. in Handbook of Elastomers, New Developments and Technology; Bhowmick, A. K.; Stephens, H. L., Eds.; Marcel Dekker: New York, 1988; p 249.
33. Dickie, R. A. J Appl Polym Sci 1973, 17, 45.
34. Holsto-Miettiner, R. M.; Seppala, J. Y.; Ikkala, O. T.; Reima, I. T. Polym Eng Sci 1994, 34, 395.
35. Kerner, E. H. Proc Phys Soc London 1956, 69B, 808.
36. Kunori, T.; Geil, P. H. J Macromol 1960, 218, 36.
37. Guth, E. J Appl Phys 1945, 16, 20.
38. Smallwood, H. M. J Appl Phys 1944, 15, 758.